Application of MPPT Techniques Using Intelligent and Conventional Control Strategies

João T. Sousa¹ and Ramiro S. Barbosa^{1,2} b

¹Department of Electrical Engineering, Institute of Engineering – Polytechnic of Porto (ISEP/IPP), 4249-015 Porto, Portugal

²GECAD - Research Group on Intelligent Engineering and Computing for Advanced Innovation and Development, ISEP/IPP, 4249-015 Porto, Portugal

Keywords: MPPT, Photovoltaic Systems, Fuzzy Logic Controller, Genetic Algorithm, P&O, Incremental Conductance,

Solar Energy.

Abstract: This paper presents a comparative study of five MPPT (Maximum Power Point Tracking) algorithms applied

to photovoltaic (PV) systems under both uniform and dynamic environmental conditions. The analyzed algorithms include two conventional methods, Perturb & Observe (P&O) and Incremental Conductance (InC), as well as a fuzzy logic controller (FLC) and two hybrid strategies enhanced by genetic algorithms (P&O+GA and InC+GA). A unified simulation framework in MATLAB/Simulink was used to ensure fair benchmarking, employing identical panel configurations, irradiance/temperature profiles, and converter parameters. Each algorithm was tested using predefined parameters such as step size, initial duty cycle, and operating bounds. Additionally, an EMA (Exponential Moving Average) filter was applied to the hybrid algorithms to reduce high-frequency measurement noise. Evaluation metrics include Mean Absolute Error (MAE), Integral Absolute Error (IAE), Mean Squared Error (MSE), Integral Squared Error (ISE), convergence time, and energy conversion efficiency. Results demonstrate that hybrid methods deliver superior performance in noisy and fast-changing conditions, while FLC maintains stable performance with reduced oscillations. This work aims to support the selection of suitable MPPT techniques for real-world PV systems, balancing computational

complexity and control effectiveness.

1 INTRODUCTION

Given the increasing global emphasis on sustainable and renewable energy solutions, photovoltaic (PV) energy plays a crucial role in the transition towards a low-carbon future. The urgency of the climate crisis, coupled with the depletion of fossil fuel reserves, has accelerated the deployment of solar technologies across diverse applications—from residential rooftops to large-scale utility plants. PV systems are particularly valued for their scalability, modularity, and ability to provide clean energy with minimal environmental impact.

The overall efficiency of a PV system is closely tied to its capability to continuously operate at the MPP (Maximum Power Point), which varies with environmental conditions such as solar irradiance, temperature, and partial shading. These factors introduce

^a https://orcid.org/0009-0000-6775-5844

^b https://orcid.org/0000-0001-7410-8872

non-linearities in the power-voltage (P–V) curve, often resulting in multiple local maximum. Under such conditions, reliably identifying and tracking the GMPP (Global Maximum Power Point) becomes a complex control problem. This challenge has made MPPT (Maximum Power Point Tracking) algorithms an indispensable component of modern PV systems.

Historically, classical MPPT methods such as Perturb & Observe (P&O) and Incremental Conductance (InC) have been favored for their simplicity and low cost. Nonetheless, they exhibit limited adaptability, oscillations around the MPP (Maximum Power Point), and suboptimal performance under dynamic or mismatched conditions. Advanced strategies including Fuzzy Logic Controllers (FLC) and hybrid approaches integrating classical methods with Genetic Algorithms (GA) have been developed to enhance convergence, minimize steady-state oscillations, and improve robustness under partial shading. This study comparatively evaluates five MPPT algo-

rithms P&O, InC, FLC, P&O+GA, and InC+GA, addressing the need for broader and more rigorous assessments as most prior works consider only a few methods under idealized conditions.

To overcome these limitations, this work delivers a thorough comparative evaluation of five widely used MPPT techniques, tested under both uniform and partial shading conditions within a unified and modular MATLAB/Simulink environment. A key strength of this study lies in the adoption of diverse performance indicators, including MAE, IAE, MSE, ISE, efficiency, and convergence time. In addition, every test condition is carefully specified in terms of irradiance and temperature, ensuring full reproducibility and transparency in the experimental methodology.

To enable a rigorous and fair comparison, a unified benchmarking strategy was adopted. All algorithms were implemented under identical simulation conditions, including converter parameters, sampling rate, and environmental inputs. The key configuration parameters defined for each algorithm, include the initial duty cycle, perturbation step size, input variables, and control structure.

The remainder of this article is structured as follows. Section 2 presents a review of the literature. Section 3 details the modeling of the photovoltaic system and simulation environment. Section 4 describes the buck converter topology and control strategy. Section 5 provides an overview of the implemented MPPT algorithms, encompassing conventional, fuzzy, and hybrid techniques. Section 6 defines the test cases, including both uniform irradiance and partial shading conditions. Section 7 introduces the performance evaluation metrics. Section 8 presents the simulation results and comparative analysis. Section 9 discusses the main findings and implications. Finally, Section 10 concludes the work and outlines possible directions for future research.

2 RELATED WORK

Recent studies have focused on improving MPPT beyond classical methods. Remoaldo and Jesus (2021) showed that integrating fuzzy logic with P&O accelerates convergence under rapid irradiance changes. Katche et al. (2023) highlighted the limitations of conventional algorithms in partial shading conditions (PSC), where multiple local maxima hinder tracking.

Aligned with this perspective, soft computing and evolutionary algorithms have gained prominence in MPPT control. According to Rezk et al. (2017), FLC (Al-Majidi et al., 2018) and adaptive neurofuzzy inference systems (ANFIS) (Belhachat and

Larbes, 2017; Mumtaz et al., 2018) effectively address the nonlinear, time-varying behavior of PV arrays. Meanwhile, bio-inspired algorithms—including GA (Shaiek et al., 2013), cuckoo search (CS) (Ahmed and Salam, 2014), ant colony optimization (ACO) (Titri et al., 2017), bee colony algorithm (BCA) (Benyoucef et al., 2015), bat-inspired optimization (BAT) (Kaced et al., 2017), and memetic salp swarm algorithm (Yang et al., 2019)—enhance GMPP detection by avoiding local optima, a key advantage under PSC and fluctuating irradiance.

Classical MPPT methods like P&O and InC are widely used for their simplicity (Lapsongphon and Nualyai, 2021; Sharma et al., 2023), but intelligent strategies such as FLC (Al-Majidi et al., 2018) improve stability. More recently, hybrid schemes with metaheuristics, especially GA (Shaiek et al., 2013; Rezk et al., 2017), have been proposed to enhance convergence under partial shading.

3 PHOTOVOLTAIC SYSTEM DESCRIPTION

The PV system models were developed in MAT-LAB/Simulink to evaluate the performance of MPPT algorithms under realistic and non-uniform conditions. Two configurations were implemented: (i) a panel with a single bypass diode, representing the actual SOLARPOWER XUNZEL 30W 24V module; and (ii) an extended model consisting of three cell groups connected in series, each with an independent bypass diode, enabling simulation of PSC.

Figure 1 illustrates the complete Simulink model used for both configurations.

The electrical characteristics of the PV panel were obtained from the manufacturer's datasheet and are listed in Table 1. These parameters were used to generate the I-V and P-V curves shown in Figure 2, with the MPP highlighted in red.

Table 1: Electrical specifications of the SOLARPOWER XUNZEL 30W 24V PV module.

Parameter	Value
Max. power (P_{max})	29.88 W
No. of cells (N_{cell})	72
Open-circuit voltage (V_{oc})	43.20 V
Short-circuit current (I_{sc})	0.92 A
Voltage at MPP (V_{mpp})	36.00 V
Current at MPP (I_{mpp})	0.83 A
Temp. coef. of $V_{oc}(\hat{\beta}_{Voc})$	−0.27 %/°C
Temp. coef. of I_{sc} (α_{Isc})	+0.05 %/°C
Temp. coef. of power (α_{Psc})	−0.35 %/°C

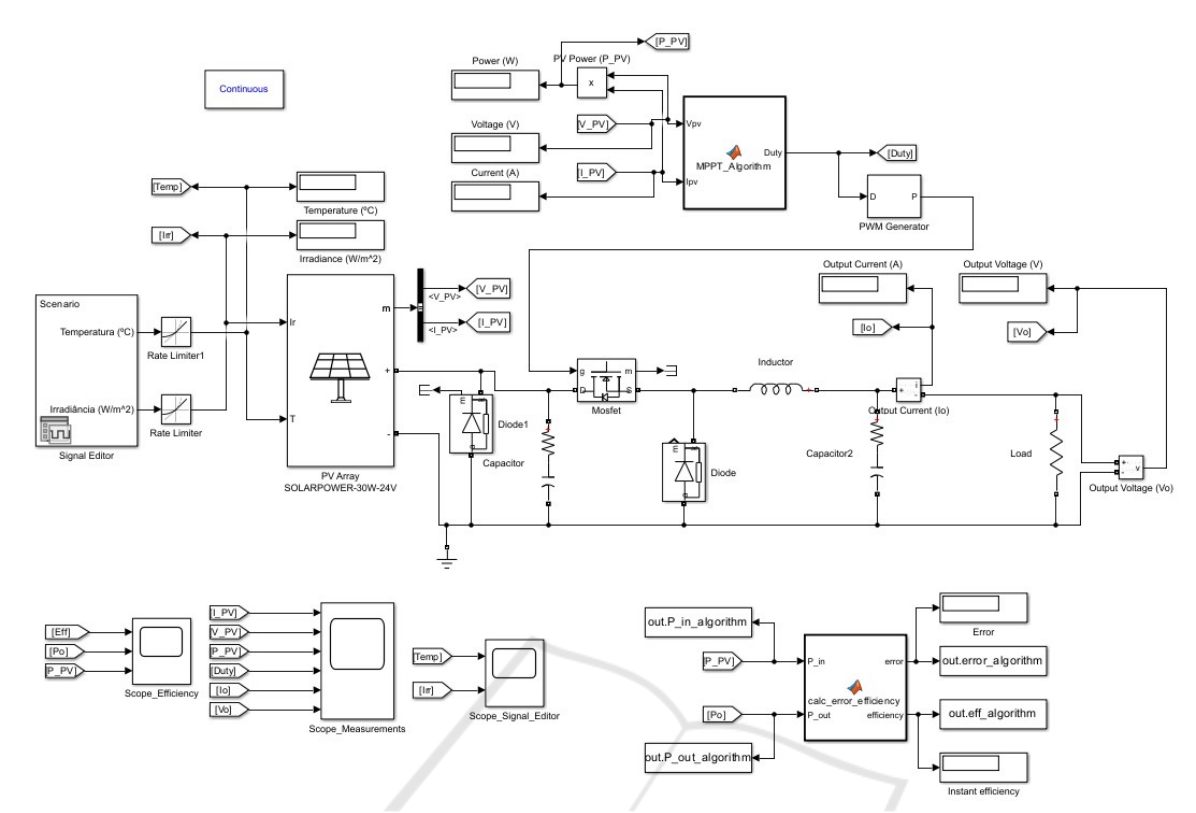


Figure 1: Simulink model of the PV system, supporting both single-diode and PSC configurations.

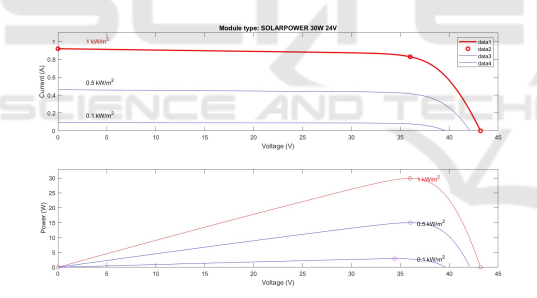


Figure 2: I-V and P-V curves of the SOLARPOWER 30W 24V panel, indicating the MPP.

4 DC/DC BUCK CONVERTER DESIGN

The DC/DC buck converter was carefully designed to interface with the PV module while ensuring operation at the MPP. The design is based on standard analytical equations, and the model was implemented in Simulink for evaluation. The electrical parameters of the PV system, summarized in Table 2, were calculated using the following equations:

$$P_{in} = V_{mpp} \times I_{mpp} \tag{1}$$

$$P_{out} = \eta \times P_{in} \tag{2}$$

$$I_{out} = \frac{P_{out}}{V_{out}} \tag{3}$$

$$V^{2}$$

$$R_o = \frac{V_{out}^2}{P_{out}} \tag{4}$$

Table 2: Calculated buck converter parameters.

Parameter	Value
Input voltage (V_{in})	36 V
Output voltage (V_{out})	20 V
Input power (P_{in})	29.88 W
Output power (P_{out})	26.89 W
Efficiency (η)	90%
MPP current (I_{mpp})	0.83 A
Output current (I_{out})	1.34 A
Load resistance (R_o)	14.88Ω

The buck converter topology is depicted in Figure 3. It consists of a controlled switch (S), a diode (D), an inductor (L), and an output capacitor (C), delivering a regulated voltage to the load (R). The input voltage from the PV module is stepped down to the desired output level $(V_{out} = 20 \text{ V})$ while maintaining the MPP operation.

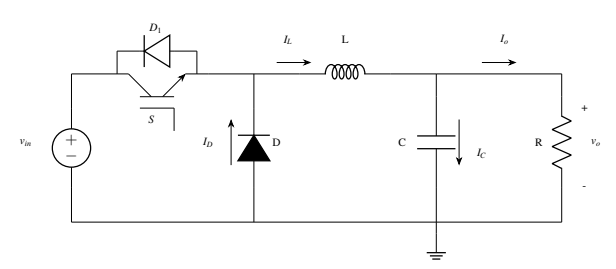


Figure 3: Topology of the DC/DC buck converter.

To ensure CCM (Continuous Conduction Mode) and maintain low ripple, the converter key parameters were derived using the following equations (Kazimierczuk and Ayachit, 2016) (Texas Instruments, 2011):

$$D = \frac{V_{out}}{V_{in}} \tag{5}$$

$$L_o \ge \frac{(V_{in} - V_{out}) \cdot D}{f_s \cdot \Delta I} \tag{6}$$

$$C_o \ge \frac{\Delta I}{8 \cdot f_s \cdot \Delta V} \tag{7}$$

Table 3 presents the final component values used in simulation.

5 MPPT ALGORITHMS OVERVIEW

This section outlines the five MPPT algorithms considered in this study, comprising two classical approaches (Perturb & Observe and Incremental Conductance), one intelligent method based on Fuzzy Logic (FL), and two hybrid strategies enhanced with GA

From a control perspective, the MPPT problem can be formalized as a regulation task where the manipulated variable is the duty cycle of the DC/DC converter, the controlled variable is the extracted PV power, and the disturbances are primarily irradiance and temperature variations. The objective is to continuously adjust the duty cycle to maintain operation at or near the MPP despite environmental changes. This viewpoint highlights MPPT as a nonlinear and timevarying control problem, where both steady-state accuracy and dynamic adaptability are crucial.

5.1 Perturb & Observe (P&O)

The Perturb & Observe (P&O) algorithm is one of the most widely adopted MPPT methods due to its simplicity and ease of implementation. This method introduces a small perturbation in the reference variable

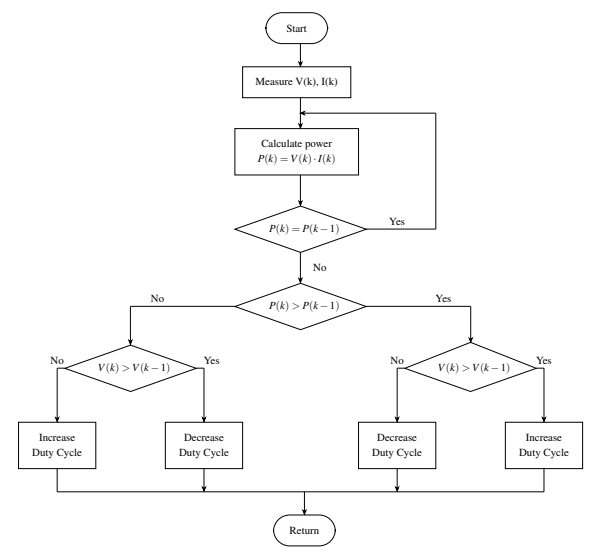


Figure 4: Flowchart of the P&O MPPT algorithm (adapted from (Lapsongphon and Nualyai, 2021)).

(typically voltage or current) and analyzes the resulting variation in output power.

The output power is computed as $P(k) = V(k) \cdot I(k)$ and compared with the previous sample. If $\Delta P = P(k) - P(k-1) > 0$, the duty cycle is adjusted in the same direction; otherwise, it is reversed. This iterative process drives the system toward the MPP (Figure 4).

In this implementation, a fixed perturbation step size of $\Delta = 1.25 \times 10^{-4}$ is used, representing the incremental change applied to the converter's duty cycle in each iteration. The initial duty cycle is set to $D_{\rm init} = 0.5555$, calculated based on the target output voltage (20 V) and the PV module's MPP voltage (36 V), using the ideal duty cycle relation $D = V_{\rm out}/V_{\rm in}$.

Previous voltage and power values $(V_{\rm old}, P_{\rm old})$ are stored to evaluate the trend of the power response. Although this method performs well under steady-state conditions, it may suffer from oscillations around the MPP and limited responsiveness under rapidly changing irradiance or temperature, due to its fixed and non-adaptive step size.

5.2 Incremental Conductance (InC)

The Incremental Conductance (InC) algorithm improves MPPT accuracy by analyzing the instantaneous slope of the P-V curve. Starting from the power expression $P = V \cdot I$, its derivative with respect to voltage is given by:

$$\frac{dP}{dV} = \frac{d(VI)}{dV} = I + V \cdot \frac{dI}{dV} \tag{8}$$

At the MPP, the derivative is zero, leading to the

Component	Value	Purpose
Duty cycle (D)	0.5555	Voltage conversion ratio
Inductor (L_o)	1658.71 μΗ	Ensures CCM for $\Delta I = 0.268 \text{ A}$
Capacitor (C_o)	1675 μF	Achieves $\Delta V = 1$ mV voltage ripple
Switching frequency (f_s)	20 kHz	Trade-off between switching losses and transient response
Current ripple (ΔI)	0.268 A	20% of I_{out} to stabilize MPPT control
Voltage ripple (ΔV)	1 mV	0.005% of V_{out} to ensure voltage precision

Table 3: Buck converter parameters used in simulations.

condition:

$$\frac{dP}{dV} = 0 \Rightarrow \frac{dI}{dV} = -\frac{I}{V} \tag{9}$$

This relation serves as the core criterion for identifying the MPP. If the condition $\frac{dI}{dV} + \frac{I}{V} = 0$ is satisfied, the system is considered to be operating at the MPP. Otherwise, the sign and magnitude of the expression determine whether the operating point lies to the left or right of the MPP.

In practical implementations, the derivatives are approximated using discrete differences as $\Delta I/\Delta V$. The algorithm then evaluates whether this approximation satisfies the MPP condition within a tolerance, i.e.,

$$\left| \frac{\Delta I}{\Delta V} + \frac{I}{V} \right| < \varepsilon \tag{10}$$

with a typical stopping threshold $\varepsilon = 10^{-6}$. If satisfied, the duty cycle remains unchanged; otherwise, it is adjusted accordingly. This logic is illustrated in the flowchart shown in Figure 5.

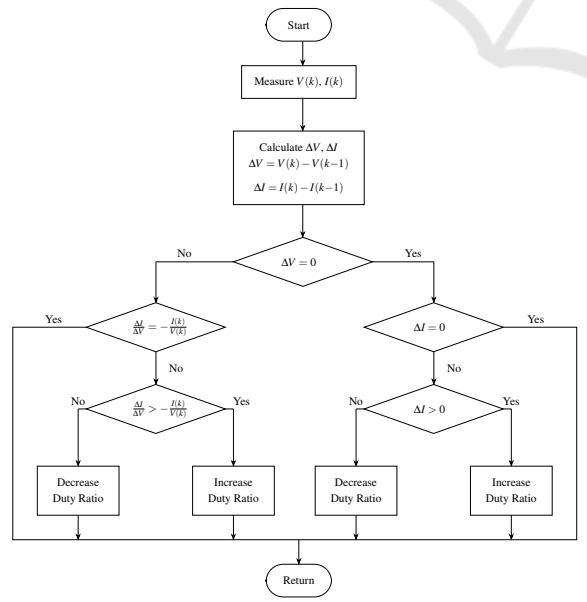


Figure 5: Flowchart of the InC MPPT algorithm (adapted from (Lapsongphon and Nualyai, 2021)).

As with P&O, this algorithm uses a fixed perturbation step size of $\Delta = 1.25 \times 10^{-4}$, an initial duty cycle $D_{\text{init}} = 0.5555$, and predefined duty bounds. However, it requires storage of previous current and voltage measurements to compute ΔI and ΔV .

Although more complex than P&O, the InC method reduces steady-state oscillations and exhibits better tracking performance under rapidly changing environmental conditions.

5.3 Fuzzy Logic Controller (FLC)

The Fuzzy Logic Controller (FLC) introduces an intelligent rule-based mechanism that emulates human decision-making in non-linear and dynamic systems. The FLC developed in this study follows the Mamdani inference model and comprises three main stages: fuzzification, rule-based inference, and defuzzification.

5.3.1 Fuzzification

Two normalized inputs are considered: the power slope error (E) and its derivative (dE), calculated as:

$$E = \frac{P(k) - P(k-1)}{V(k) - V(k-1)}, \quad dE = E(k) - E(k-1)$$
(11)

These quantities are normalized to the [-1,1] range using saturation functions:

$$E_{\text{norm}} = \text{sat}\left(\frac{E}{0.5}\right), \quad dE_{\text{norm}} = \text{sat}\left(\frac{dE}{0.2}\right) \quad (12)$$

Triangular membership functions are employed for both inputs, dividing the universe of discourse into five linguistic labels (Figure 6): Negative Large (NL), Negative Small (NS), Zero (Z), Positive Small (PS), and Positive Large (PL). These functions are defined by:

$$\mu(x, a, b, c) = \max\left(\min\left(\frac{x - a}{b - a}, \frac{c - x}{c - b}\right), 0\right) \quad (13)$$

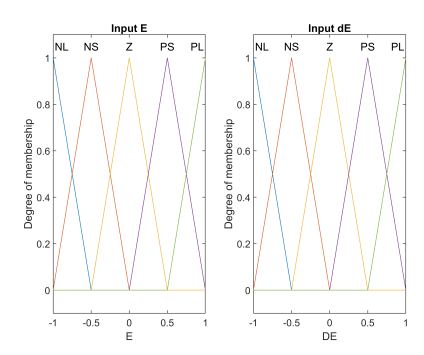


Figure 6: Triangular membership functions for the input variables: error (E) and derivative of the error (dE).

Listing 1: Mamdani implication operator in code.

w = min(muE(i), muDE(i));

5.3.2 Inference Mechanism

The fuzzy rule base is built on a 5×5 grid, mapping the combinations of E and dE to the variation in duty cycle ΔD . The Mamdani inference method is applied, using the min operator to determine the activation weight of each rule:

Table 4 shows the complete rule base used to define the control actions.

Table 4: Fuzzy rule base for ΔD (duty cycle variation) using linguistic variables.

E dE	NL	NS	Z	PS	PL
NL	PL	PL	PS	PS	Z
NS	PL	PS	PS	Z	NS
Z	PS	Z	Z	Z	NS
PS	Z	NS	NS	NS	NL
PL	NS	NS	NL	NL	NL

Examples of rule definitions include:

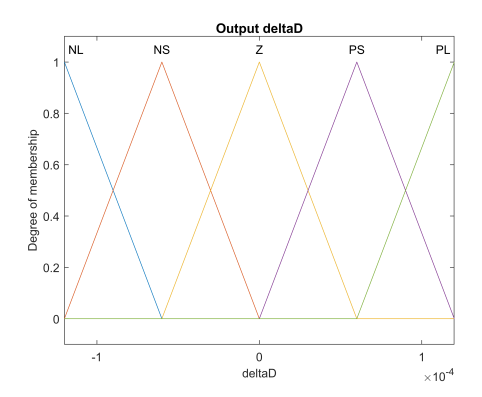
- IF E is NL AND dE is NL THEN ΔD is PL
- IF E is Z AND dE is Z THEN ΔD is Z
- IF E is PL AND dE is PL THEN ΔD is NL

This configuration ensures that strong deviations from the MPP lead to larger duty cycle adjustments, whereas near-optimal conditions result in smaller or null changes, promoting stability.

The rule base values ΔD_{ij} and the associated weights w_{ij} determine the fuzzy output surface, which is visualized in Figure 7.

5.3.3 Defuzzification

The defuzzification stage employs the Center of Gravity (COG) method, which computes the crisp output



(a) Output membership functions

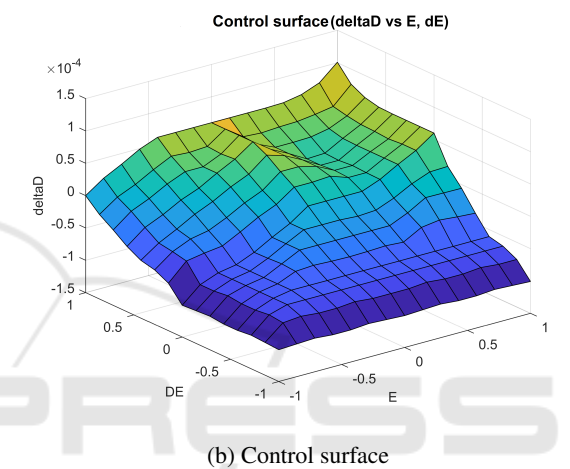


Figure 7: (a) Output fuzzy sets for ΔD and (b) resulting fuzzy control surface.

as the weighted average of all rule consequences:

$$\Delta D_{\text{output}} = \frac{\sum_{i=1}^{5} \sum_{j=1}^{5} w_{ij} \cdot \Delta D_{ij}}{\sum_{i=1}^{5} \sum_{j=1}^{5} w_{ij}}$$
(14)

where:

- $w_{ij} = \min(\mu_E(i), \mu_E(j))$ is the rule activation weight;
- ΔD_{ij} is the output action for rule (i, j) based on the fuzzy rule base.

The FLC provides effective tracking of the MPP under varying irradiance and temperature, with lower oscillations compared to conventional methods, albeit with slightly increased computational complexity due to rule evaluation and inference mechanisms.

5.4 Hybrid Algorithms (InC+GA and P&O+GA)

Hybrid approaches integrate classical MPPT techniques (P&O and InC) with Genetic Algorithms (GA) to overcome the limitations of fixed step size and improve adaptability under complex environmental scenarios.

In both hybrids, the GA dynamically optimizes the perturbation step size Δ within a bounded range of [0.00005, 0.0002], aiming to maximize output power while minimizing high-frequency oscillations. The fitness function is defined as:

Fitness =
$$V_{pv} \cdot I_{pv} - 5 \cdot \Delta$$
 (15)

where the penalty term ensures that smaller step sizes are favored if they maintain high power output.

The configuration of the GA used for step-size optimization in both hybrid methods is summarized in Table 5.

Table 5: Genetic Algorithm parameters used in hybrid MPPT approaches.

Parameter	Value
Population size	50 individuals
Number of generations	5
Selection method	Tournament (size $= 3$)
Crossover type	Random factor α
Mutation rate	30%

An exponential moving average (EMA) filter is applied to voltage and current measurements to suppress measurement noise (Martins et al., 2019)(Tajiri and Kumano, 2012):

$$x_f(k) = \alpha \cdot x(k) + (1 - \alpha) \cdot x_f(k - 1) \tag{16}$$

where x represents the measured signals V_{pv} and I_{pv} , and $\alpha = 0.01$ is the smoothing coefficient.

The hybrid P&O+GA algorithm retains the standard perturbation logic but applies the optimized Δ_{opt} from GA at each cycle, as illustrated in the flowchart in Figure 8. Similarly, InC+GA applies the incremental conductance logic, using the GA-tuned step size.

These hybrid methods significantly enhance tracking performance, particularly under PSC, achieving high efficiency with minimal error metrics.

5.5 Benchmarking Configuration

To ensure a rigorous and equitable assessment of all MPPT algorithms presented in this work, a unified benchmarking methodology was employed. Each algorithm was implemented within the same simulation environment, leveraging identical photovoltaic and

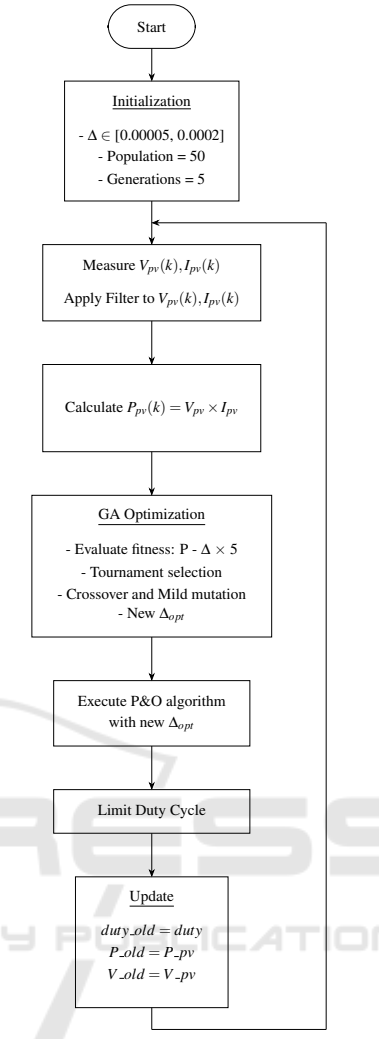


Figure 8: Flowchart of the GA+P&O algorithm.

converter models, input profiles, and sampling conditions. Table 6 details the core configuration parameters defined for each strategy, including the initial duty cycle, perturbation step size, control approach, and required input signals.

6 SIMULATION SCENARIOS

To evaluate the performance of the implemented MPPT algorithms under realistic operating conditions, a subset of representative scenarios was selected from a broader test set. This selection balances coverage of typical, dynamic, and critical operating conditions while maintaining compactness suitable for the scope of this paper.

Two types of scenarios were considered: (i) conventional operating conditions with a single bypass

Algorithm	Step Size (adimensional, duty cycle step) Δ	D_{init}	Bounds	Tuning	Inputs (Volts, Amperes)
P&O	1.25×10^{-4}	0.5555	0/1	Fixed	V_{pv}, I_{pv}
InC	1.25×10^{-4}	0.5555	0/1	Fixed	V_{pv}, I_{pv}
FLC	N/A	N/A	0/1	Rules	V_{pv}, I_{pv}
InC+GA	$[5.0 \times 10^{-5}, 2.0 \times 10^{-4}]$	0.5555	0/1	GA	V_{pv}, I_{pv}
P&O+GA	$[5.0 \times 10^{-5}, 2.0 \times 10^{-4}]$	0.5555	0/1	GA	V_{pv}, I_{pv}

Table 6: Algorithm configuration parameters.

diode, and (ii) PSC with three bypass diodes, each protecting a series-connected group of cells.

Table 7 summarizes the selected cases for the single bypass diode configuration, including one ideal (uniform) and one dynamic case with simultaneous variation of irradiance and temperature.

Table 7: Selected scenarios with single bypass diode.

Case	Scenario Description	Fixed Parameters
S1	Uniform irradiance: $G = 1000 \text{ W/m}^2$	$T = 25^{\circ} \text{C}$
S2	Simultaneous variation of <i>G</i> and <i>T</i>	T a

Figures 9 and 10 illustrate the irradiance and temperature profiles for scenarios S1 and S2, respectively. Scenario S1 represents a constant and ideal condition, while S2 reflects a more realistic and challenging case with time-varying environmental conditions.

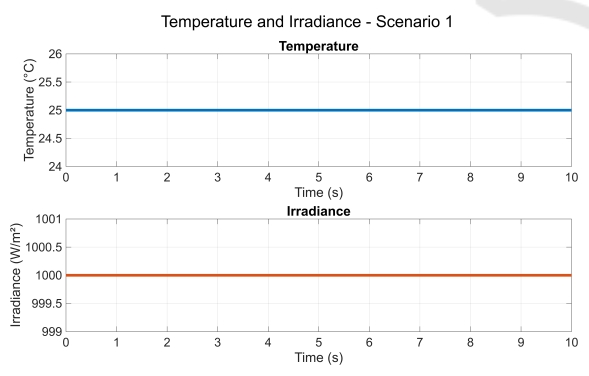


Figure 9: Irradiance and temperature profile for scenario S1 (uniform condition).

Table 8 presents the selected PSC cases with three cell groups, each affected by different irradiance values. Case S3 represents a moderately mismatched condition with one shaded group, while Case S4 corresponds to a severely mismatched configuration with all groups shaded at different levels.

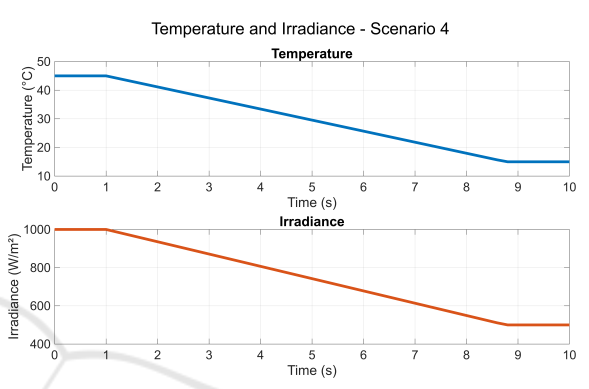


Figure 10: Irradiance and temperature variation for scenario S2 (dynamic condition with environmental changes over time).

Table 8: Selected PSC scenarios with three bypass diodes.

Case	PSC Configuration	Fixed Parameters
S3	G =	$T = 25^{\circ}\text{C}$
	[900, 1000, 200]	
	W/m^2	
S4	G = [300, 200, 100]	$T = 25^{\circ} \text{C}$
	W/m ²	

Figures 11 and 12 show the irradiance conditions for scenarios S3 and S4, respectively.

7 EVALUATION METRICS

To rigorously evaluate the behavior of the MPPT algorithms under diverse operating scenarios, a set of six performance indicators was selected. These metrics enable a multi-dimensional assessment by capturing key aspects such as tracking accuracy, transient behavior, stability, and overall energy efficiency.

7.1 Error-Based Indicators

Four distinct error metrics were adopted to quantify the deviation between the theoretical maximum input

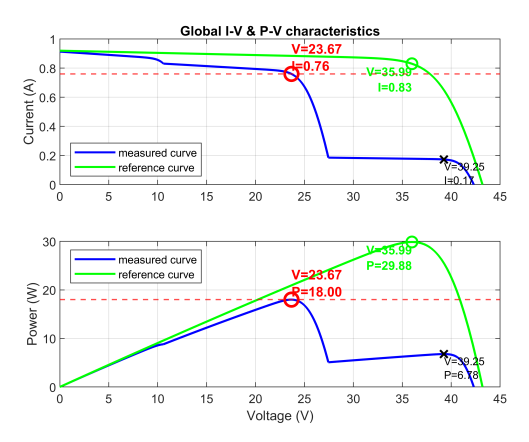


Figure 11: Irradiance profile for scenario S3 (moderate partial shading with one significantly shaded cell group).

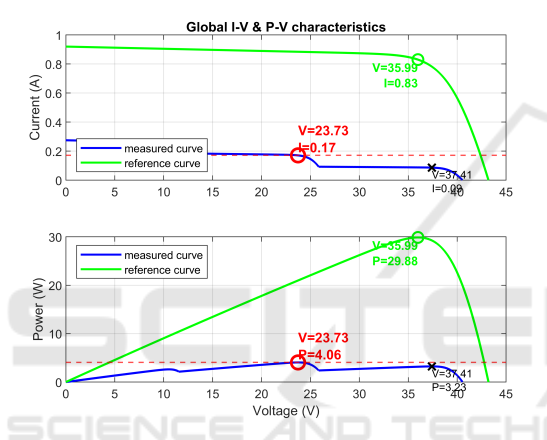


Figure 12: Irradiance profile for scenario S4 (severe mismatch, with all three groups under different shading conditions).

power provided by the PV panel (P_{in}) and the actual output power extracted by the converter (P_{out}) :

• Mean Absolute Error (MAE): Represents the average magnitude of the absolute error over the entire simulation interval:

$$MAE = \frac{1}{N} \sum_{t=1}^{N} |P_{in}(t) - P_{out}(t)|$$
 (17)

where N is the total number of samples. Lower MAE values reflect better steady-state precision.

• **Integral Absolute Error (IAE):** Measures the accumulated absolute deviation over time, highlighting sustained tracking inaccuracies:

IAE =
$$\int_{0}^{T} |P_{in}(t) - P_{out}(t)| dt$$
 (18)

Particularly sensitive to long-term error persistence, IAE is useful for evaluating algorithmic robustness during transitions.

 Mean Squared Error (MSE): Weighs deviations more heavily by squaring the instantaneous errors, thus penalizing larger discrepancies:

$$MSE = \frac{1}{N} \sum_{t=1}^{N} [P_{in}(t) - P_{out}(t)]^{2}$$
 (19)

• **Integral Squared Error (ISE):** Integrates the squared error over time, offering insight into the temporal distribution of large tracking deviations:

ISE =
$$\int_{0}^{T} [P_{in}(t) - P_{out}(t)]^{2} dt$$
 (20)

This metric is especially pertinent in scenarios such as partial shading, where abrupt power fluctuations are more common.

7.2 Efficiency and Transient Response Metrics

In addition to tracking accuracy, the energy extraction capability and dynamic response were assessed through the following indicators:

 Energy Conversion Efficiency (η): Assesses the algorithm's effectiveness in harnessing the available power:

$$\eta = \left(\frac{\overline{P_{out}}}{\overline{P_{in}}}\right) \times 100\% \tag{21}$$

where \overline{P} denotes the average power over the observation period.

• Convergence Time (t_{conv}): Refers to the time taken for the system to reach and consistently maintain steady-state operation. This parameter was determined using MATLAB's lsiminfo function, with a settling threshold of 2%. Additional validation was performed through a moving average analysis of the power error signal to ensure robustness against transient oscillations.

8 RESULTS

This section presents a comparative analysis of five MPPT algorithms under distinct environmental conditions. The selected algorithms include two classical techniques, Perturb & Observe (P&O) and Incremental Conductance (InC), a fuzzy logic-based controller (FLC), and two hybrid approaches enhanced by genetic algorithms (P&O+GA and InC+GA). Performance was assessed using six key metrics: MAE, MSE, IAE, ISE, average efficiency (%), and convergence time (s).

8.1 Scenario S1 – Constant Irradiance and Temperature

In this baseline scenario (1000 W/m², 25°C), the hybrid controllers outperformed the classical techniques by a significant margin. As shown in Table 9, InC+GA and P&O+GA presented the lowest MSE values (2.76), and reduced cumulative errors (IAE and ISE), indicating precise and consistent tracking. The FLC also delivered competitive results, with a notable efficiency of 95.37% and fast convergence. Conversely, P&O and InC showed higher steady-state errors and lower efficiencies, confirming their limited optimization capability under steady conditions.

Table 9: Performance metrics – Scenario S1 (1000 W/m², 25°C).

Algorithm	MAE (W)			ISE (W ² ·s)	Eff. (%)	Time (s)
P&O	2.27	8.45	23.65	96.78	93.60	0.20
InC	2.27	8.42	23.65	96.77	93.63	0.20
FLC	1.30	3.49	13.57	45.56	95.37	0.24
InC+GA	1.31	2.76	13.64	33.88	95.31	0.38
P&O+GA	1.31	2.76	13.64	33.86	95.32	0.38

Furthermore, the convergence behaviors of the advanced approaches are illustrated in Figures 13, 14, 15, showing a smooth and fast reduction in the error between P_{in} and P_{out} , with minimal oscillations. These results reinforce the superior dynamic response observed in the quantitative metrics.

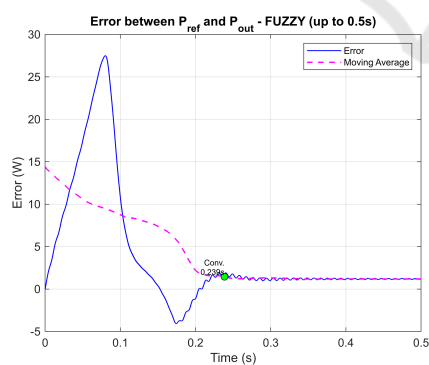


Figure 13: Error between P_{ref} and P_{out} for the FLC algorithm under Scenario S1, highlighting convergence time.

8.2 Scenario S2 – Variable Irradiance and Temperature

Under simultaneous fluctuations in irradiance and temperature, the system's dynamic behavior plays a critical role in MPPT effectiveness. As reported in Table 10, the hybrid algorithms maintained strong

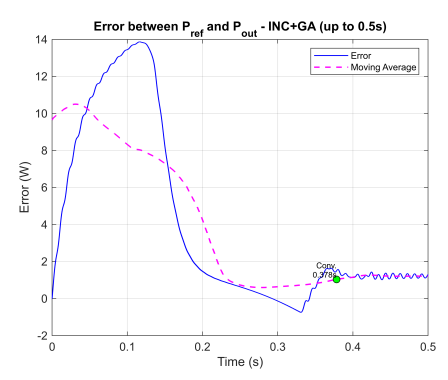


Figure 14: Error between P_{ref} and P_{out} for the InC+GA algorithm under Scenario S1, highlighting convergence time.

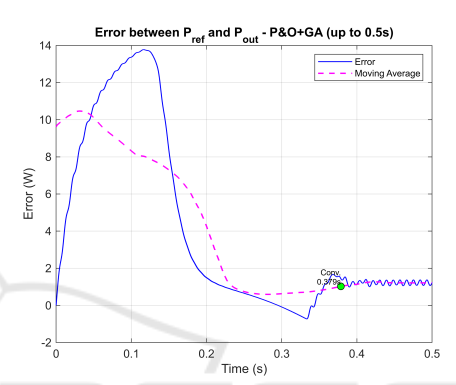


Figure 15: Error between P_{ref} and P_{out} for the P&O+GA algorithm under Scenario S1, highlighting convergence time.

performance with MAE values around 1.26 and high efficiencies close to 94%. FLC again showed good adaptation with reduced tracking errors and a moderate convergence time. Traditional methods lagged behind, exhibiting slower response and reduced efficiency due to their limited adaptability to non-linear environmental variations.

Table 10: Performance metrics – Scenario S2 (variable G and T).

Algorithm	MAE (W)	MSE (W ²)	IAE (W·s)	ISE (W ² ·s)	Eff. (%)	Time (s)
P&O	1.91	6.33		71.38		
InC	1.88	6.23	19.54	71.49	92.57	0.19
FLC	1.23	3.07	12.70	38.77	94.05	0.23
InC+GA	1.26	2.84	13.00	33.07	93.87	0.37
P&O+GA	1.26	2.84	12.99	33.19	93.89	0.37

8.3 Scenario S3 – Partial Shading (Moderate)

Partial shading introduces local maximum in the power-voltage curve, making it particularly challenging for conventional MPPT techniques. In this moderate PSC scenario ($G = [900, 1000, 200] \text{ W/m}^2$), hy-

brid methods clearly surpassed classical algorithms, as shown in Table 11. Both InC+GA and P&O+GA reached high efficiency levels (96.22%), while FLC achieved the lowest MAE (0.62), confirming its suitability for non-linear operating profiles. Classical methods failed to monitoring local maximum, resulting in increased tracking errors.

Table 11: Performance metrics – Scenario S3 (PSC: [900, 1000, 200] W/m²).

Algorithm	MAE (W)	MSE (W ²)		ISE (W ² ·s)	Eff. (%)	Time (s)
P&O	1.25	2.46	12.80	27.07	94.39	0.23
InC	1.25	2.46	12.80	27.08	94.39	0.23
FLC	0.62	0.89	6.46	11.11	96.30	0.19
InC+GA	0.64	0.77	6.58	9.57	96.22	0.41
P&O+GA	0.64	0.76	6.58	9.52	96.22	0.41

8.4 Scenario S4 – Partial Shading (Severe)

The final test scenario introduces extreme partial shading (G = [300, 200, 100] W/m²), producing multiple local maximum in the P-V curve. Table 12 highlights the superior reliability of the hybrid methods, with both InC+GA and P&O+GA yielding efficiencies near 92% and significantly lower error indices (MAE \approx 0.20). In contrast, classical and FLC-based methods failed to maintain optimal tracking, with overall efficiencies around 85%. These results confirm the hybrid strategies resilience and accuracy under highly non-uniform operating conditions.

Table 12: Performance metrics – Scenario S4 (PSC: [300, 200, 100] W/m²).

Algorithm	MAE (W)	MSE (W ²)	IAE (W·s)	ISE (W ² ·s)	Eff. (%)	Time (s)
P&O	0.58	0.57	6.18	6.40	85.55	0.38
InC	0.60	0.58	6.17	6.40	85.18	0.38
FLC	0.55	0.38	5.65	4.13	85.69	0.53
InC+GA	0.20	0.05	2.02	0.52	91.95	0.40
P&O+GA	0.20	0.05	2.03	0.56	91.93	0.40

9 DISCUSSION

The comparative results across Scenarios S1 to S4 reveal distinct performance trends among the tested MPPT algorithms. Classical methods like P&O and InC demonstrated consistent behavior and low implementation complexity but were limited in adaptability, particularly under dynamic and partial shading conditions. Their tracking precision degraded in Sce-

narios S2, S3, and S4, often failing to reach the global maximum.

The FLC provided improved accuracy and stability in both uniform and moderately variable conditions. Its rule-based structure enabled better adaptability than conventional algorithms. However, struggled to accurately track the global peak under severe partial shading (Scenario S4).

Hybrid approaches enhanced with genetic algorithms (P&O+GA and InC+GA) consistently delivered the best overall results. These methods showed high efficiency, minimal error metrics, and strong resilience under complex conditions, particularly in the PSC scenarios.

Table 13 summarizes the main characteristics of the five MPPT algorithms evaluated in this study.

10 CONCLUSIONS

This work presented a comprehensive comparative analysis of five MPPT algorithms, P&O, InC, FLC, P&O+GA, and InC+GA, evaluated under uniform, dynamic, and partial shading conditions through a unified MATLAB/Simulink framework. Results demonstrated that hybrid methods enhanced by genetic algorithms consistently outperform conventional and fuzzy logic controllers, delivering superior efficiency, accuracy, and resilience, particularly under severe partial shading. The FLC showed reliable tracking with reduced oscillations in moderately variable conditions, while classical methods exhibited limited adaptability, especially under complex operating scenarios.

A natural progression of this research involves the integration of a bidirectional DC/DC converter, specifically a Buck-Boost topology, which would enable both charging and discharging of an energy storage system. This architecture would facilitate the transition from a passive PV system to a hybrid energy management solution, capable of supplying loads autonomously during periods of low solar generation.

Additionally, future work could focus on the experimental validation of the proposed MPPT algorithms under real-world operating conditions. This would involve developing a physical prototype that integrates photovoltaic panels, bidirectional converters, embedded controllers (e.g., microcontroller), and appropriate sensors for current, voltage, irradiance, and temperature measurement. Implementing the control logic directly in embedded hardware would allow for the assessment of real-time performance, computational constraints, and resilience to distur-

Algorithm	Complexity	Cony. Speed	Stability	Adapability	PSC Perf.	Şensors
P&O	Low	Fast	Low	Low	Weak	V, I
InC	Medium	Fast	Low	Low	Weak	V, I
FLC	High	Medium	High	Medium	Good	V, I
P&O+GA	High	Medium	High	High	V.Good	V, I
InC+GA	High	Medium	High	High	V.Good	V, I

Table 13: Qualitative comparison of MPPT algorithms.

bances such as measurement noise or sudden environmental changes.

REFERENCES

- Ahmed, J. and Salam, Z. (2014). A maximum power point tracking (mppt) for pv system using cuckoo search with partial shading capability. *Applied Energy*, 119:118–130.
- Al-Majidi, S. D., Abbod, M. F., and Al-Raweshidy, H. S. (2018). A novel maximum power point tracking technique based on fuzzy logic for photovoltaic systems. *International Journal of Hydrogen Energy*, 43(31):14158–14171.
- Belhachat, F. and Larbes, C. (2017). Global maximum power point tracking based on anfis approach for pv array configurations under partial shading conditions. *Renewable and Sustainable Energy Reviews*, 77:875–889.
- Benyoucef, A. s., Chouder, A., Kara, K., Silvestre, S., and sahed, O. A. (2015). Artificial bee colony based algorithm for maximum power point tracking (mppt) for pv systems operating under partial shaded conditions. *Applied Soft Computing*, 32:38–48.
- Kaced, K., Larbes, C., Ramzan, N., Bounabi, M., and Dahmane, Z. e. (2017). Bat algorithm based maximum power point tracking for photovoltaic system under partial shading conditions. *Solar Energy*, 158:490–503.
- Katche, M. L., Makokha, A. B., Zachary, S. O., and Adaramola, M. S. (2023). A comprehensive review of maximum power point tracking (mppt) techniques used in solar pv systems. *Energies*, 16(5):2206.
- Kazimierczuk, M. K. and Ayachit, A. (2016). Laboratory manual for pulse-width modulated dc-dc power converters, second edition. Laboratory manual supplementing the second edition of the textbook.
- Lapsongphon, C. and Nualyai, S. (2021). A comparison of mppt solar charge controller techniques: A case for charging rate of battery. pages 278–281.
- Martins, J., Spataru, S., Sera, D., Stroe, D.-I., and Lashab, A. (2019). Comparative study of ramp-rate control algorithms for pv with energy storage systems. *Energies*, 12(7):1342.

- Mumtaz, S., Ahmad, S., Khan, L., Ali, S., Kamal, T., and Hassan, S. (2018). Adaptive feedback linearization based neurofuzzy maximum power point tracking for a photovoltaic system. *Energies*, 11(3):606.
- Remoaldo, D. and Jesus, I. (2021). Analysis of a traditional and a fuzzy logic enhanced perturb and observe algorithm for the mppt of a photovoltaic system. *Algorithms*, 14(1):24.
- Rezk, H., Fathy, A., and Abdelaziz, A. Y. (2017). A comparison of different global mppt techniques based on meta-heuristic algorithms for photovoltaic system subjected to partial shading conditions. *Renewable and Sustainable Energy Reviews*, 74:377–386.
- Shaiek, Y., Ben Smida, M., Sakly, A., and Mimouni, M. F. (2013). Comparison between conventional methods and ga approach for maximum power point tracking of shaded solar pv generators. *Solar Energy*, 90:107–122.
- Sharma, A. K., Pachauri, R. K., Choudhury, S., Minai, A. F., Alotaibi, M. A., Malik, H., and Márquez, F. P. G. (2023). Role of metaheuristic approaches for implementation of integrated mppt-pv systems: A comprehensive study. *Mathematics*, 11(2):269.
- Tajiri, H. and Kumano, T. (2012). Input filtering of mppt control by exponential moving average in photovoltaic system. pages 372–377.
- Texas Instruments (2011). Basic calculation of a buck converter's power stage (rev. b). Application Report, revised July 2011.
- Titri, S., Larbes, C., Toumi, K. Y., and Benatchba, K. (2017). A new mppt controller based on the ant colony optimization algorithm for photovoltaic systems under partial shading conditions. *Applied Soft Computing*, 58:465–479.
- Yang, B., Zhong, L., Zhang, X., Shu, H., Yu, T., Li, H., Jiang, L., and Sun, L. (2019). Novel bio-inspired memetic salp swarm algorithm and application to mppt for pv systems considering partial shading condition. *Journal of Cleaner Production*, 215:1203–1222.